SAND2007-2656C

VACUUM ARC REMELTING POOL POWER CONTROL

Joseph J. Beaman[a], Rodney L. Williamson[b], David K. Melgaard[b], Robert M. Aikin, Jr.[c], and Robert G. Erdmann[d]

[a]Department of Mechanical Engineering, University of Texas at Austin, Texas, U.S.A.

[b] Joining and Coating Department, Sandia National Laboratories, Albuquerque, New Mexico, U.S.A

[c]Materials Science and Technology: Metallurgy, Los Alamos National Laboratory, Los Alamos, New Mexico, U.S.A

[d]Department of Materials Science and Engineering, University of Arizona, Tucson, Arizona, U.S.A.

Abstract

Modern methods of controlling a vacuum arc remelting (VAR) process focus on controlling electrode gap and either melting current or electrode melt rate. Current control has the advantage of simplicity. In this method, the melting current is made to follow a preset schedule using a current feedback loop. This method specifies the total electrical arc power during steady-state operation. On the other hand, controlling melt rate specifies the power carried into the ingot from dripping molten metal. Under circumstances where the process encounters transients, such as melting though electrode cracks or welds, the ratio of power input into the ingot from the arc and molten metal shifts even though the current or electrode melt rate is held constant. Ingot simulations indicate that this shift in power distribution perturbs the solidification interface. We have developed an alternative method of VAR control which aims at controlling the total power into the top of the ingot. Simulation work shows that this method does a better job at controlling perturbations to the ingot solidification zone. Preliminary tests using a laboratory scale VAR furnace to melt 150 mm diameter 304 stainless steel electrodes into 200 mm diameter ingots show promising results.

I. Introduction

Vacuum arc remelting (VAR) is a common process used throughout the specialty metals industry for controlled casting of segregation sensitive and reactive metal alloy ingots. In normal industrial practice, several process variables are monitored and controlled in order to consistently create high quality ingots. The most common form of VAR process control seeks to control process current and electrode gap. Typically, process current is controlled to a reference set-point using a PI or PID control feedback loop. Electrode gap is usually controlled by maintaining the process either to a reference voltage or a reference drip-short frequency. Either method is based on the assumption that the electrode gap will be controlled to a constant value if the process is forced to faithfully track the voltage or drip-short frequency reference.

Another important process variable is electrode melt rate. Variations cause transients in the ingot growth rate and mushy zone thermal gradient, a condition conducive to the formation of melt related defects.[1] For example, such transients have been linked to freckle formation[2] in nickel-base superalloys, as well as solidification white spot formation in Alloy 718.[3] It is thought that controlling melt rate during transient melting and through common melt rate disturbances could lead to significant improvements in product yields as well as reduce the number of melt related defects in segregation sensitive alloys.[4] Melt rate control involves controlling electrode gap and electrode melting rate instead of electrode gap and process current. In this system, process current is made to be whatever it needs to be in order to meet the melt rate reference. A control technique to achieve dynamic melt rate control is described in Williamson, et al.[5]

Both current and melt rate control methods have advantages and disadvantages. Current control has the advantage of simplicity. In this method, the melting current is made to follow a preset schedule using a feedback loop. Assuming a constant electrode gap and stable furnace atmosphere, this method controls the total electrical arc power during steady-state operation. On the other hand, controlling melt rate controls the energy carried into the ingot from enthalpy in the dripping molten metal. Typically, both methods utilize drip-short frequency or process voltage as a ram velocity feedback variable to control electrode gap. Under circumstances where the process encounters transients, such as minor glows or when melting though electrode cracks or welds, the ratio of power input into the ingot from the arc and molten metal shifts even though the total arc power or electrode melt rate is held constant. Ingot simulations indicate that this shift in energy distribution perturbs the solidification interface. We have developed an alternative method of VAR control which aims at controlling the total power into the ingot. This method uses the melting current to simultaneously adjust the arc power and melt rate so that the total power from these two sources is controlled to a set-point.

In Section II of this paper, the basic equations underlying pool power control and its control architecture are presented. Section III describes the results of a simulation study that compares the differences of current control, melt rate control, and pool power control during a simulated melting of a cracked electrode. Section IV describes controller tests carried out at the MST Foundry at Los Alamos National Laboratory, and conclusions are presented in Section V.

II. Pool Power Control Architecture

Pool power is a new method of VAR process control that has the goal of controlling the power to the top of the ingot surface. For steady state melting, all of the control methods are identical, but it is hypothesized that this type of control will be superior to either current control or melt rate control during transient events. Pool power represents the energy boundary condition at the top surface of the ingot and it seems logical that keeping this boundary condition constant during the VAR process might lead to more uniform ingots. Pool power controller development makes the following assumptions: 1) a uniform, diffuse arc exists throughout the inter-electrode region; 2) contributions to changes in pool power due to radiation may be neglected; 3) melting power returns to the pool as enthalpy contained in the molten metal dripping from the electrode; and 4) current arc plasma power is distributed between the pool and ingot wall above the pool according to simple geometry. Given these assumptions, the following equation may be derived describing the pool power:

$$P_{pool} = \frac{\dot{m} h_{\sup}}{\rho} + \varepsilon \left[V_{CF} I + \left(R_I + R_G G \right) I^2 \right]. \qquad (1)$$

In this equation, $\dot{m}$ is electrode melt rate, ρ is density at superheat temperature, $h_{\sup}$ is volume specific enthalpy at superheat temperature, ε is arc power fraction to the pool surface, V_{CF} is the cathode fall voltage, I is the process current, R_I is the VAR circuit resistance less the electrode gap resistance, R_G is the experimentally determined electrode gap resistance parameter, and G is electrode gap.

The melt rate is determined by a reduced order model that is described in Beaman[6] and is given by the solution of the following two nonlinear equations

$$\dot{m} = -\frac{\rho A_e \alpha_r C_{s\Delta}}{\Delta} + \frac{\rho C_{sp} \mu \left[V_{CF} I + \left(R_I + R_G G \right) I^2 \right]}{h_m} \qquad (2)$$

$$\dot{\Delta} = \frac{\alpha_r C_{\Delta\Delta}}{\Delta} - \frac{C_{\Delta p} \mu \left[V_{CF} I + (R_I + R_G G) I^2 \right]}{h_m A_e} \qquad (3)$$

where A_e is electrode cross-sectional area, α_r is room temperature thermal diffusivity, $C_{s\Delta}$ and C_{sp} are non-dimensional material dependent constants, μ is process efficiency (the fraction of power going into melting the electrode to the total process power), Δ is electrode thermal boundary layer, and h_m is volume specific enthalpy at melt temperature. Note that the quantity enclosed in square brackets in these expressions defines the total process power. This quantity multiplied by ε gives the fraction of the total power collected at the pool surface from the arc plasma. Thus, Equation (1) simply states that the pool power is equal to the total enthalpy input due to the melting electrode plus the total arc plasma power collected by the pool surface. If Equation (2) is substituted into Equation (1) and the result solved for current, the pool power control equation is obtained:

$$I = \frac{-V_{CF}}{2\left(R_I + R_G G\right)} + \sqrt{\left(\frac{V_{CF}}{2\left(R_I + R_G G\right)} \right)^2 + \frac{P_{pool} + \dfrac{\alpha_r C_{s\Delta} A_e h_{\sup}}{\Delta}}{\left(\dfrac{\mu C_{sp} h_{\sup}}{h_m} + \varepsilon \right)\left(R_I + R_G G\right)}}. \qquad (4)$$

This equation may be used to find the current required to give pool power P_{pool}. A nonlinear controller can be designed around Equation (4). The result is very similar to the melt rate controller described in Williamson et al[5] except that the reference inputs are G_{ref} and $P_{pool,ref}$ instead of G_{ref} and $\dot{m}_{ref}$. The process input commands are still the commended current I_c and commanded electrode ram speed $U_{ram,c}$ or commanded ram position $X_{ram,c}$. A schematic diagram of the controller is shown in Figure 1. The VAR estimator for this controller is identical to that of the melt rate controller.

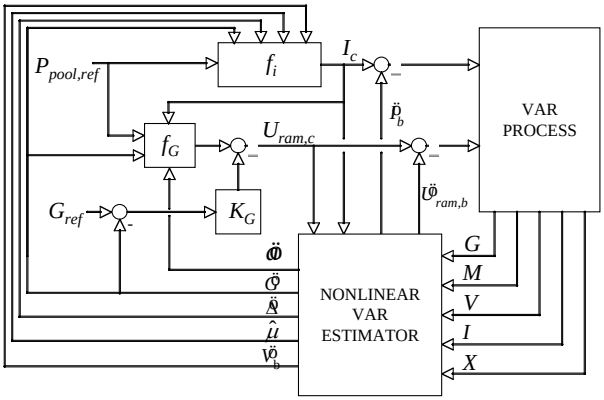

Figure 1: Schematic of Pool Power controller

The function boxes f_I and f_G in Figure 1 are defined below. A hat over a variable indicates an estimated quantity.

$$f_I = \frac{-\left(V_{CF} + \hat{V}_b\right)}{2\left(R_I + R_G \hat{G}\right)} + \sqrt{\left(\frac{V_{CF} + \hat{V}_b}{2\left(R_I + R_G \hat{G}\right)} \right)^2 + \frac{P_{pool,ref} + \dfrac{\alpha_r C_{s\Delta} h_{\sup}}{\hat{\Delta}}}{\left(\dfrac{\hat{\mu} C_{sp} h_{\sup}}{h_m} + \varepsilon \right)\left(R_I + R_G \hat{G}\right)}} \qquad (4)$$

$$f_G = \frac{\hat{a}}{h_{\sup} A_e}\left\{P_{pool,ref} - \varepsilon\left[\left(V_{CF} + \hat{V}_b\right) I_c + \left(R_I + R_G G\right) I_c^2\right]\right\} \quad (5)$$

$\hat{V}_b$ in these equations is the estimated voltage bias. Likewise, $\hat{I}_b$ and $\hat{U}_{ram,b}$ in Figure 1 are estimated current bias and ram velocity bias, respectively. The bias terms are included to improve steady state controller accuracy. They do not change the overall structure of the pool power controller. For a VAR furnace with unbiased current and ram speed control and unbiased values for the electrical parameters V_{CF}, R_I, and R_G, the bias terms are equal to zero.

III. Simulation Comparison of Current, Melt Rate, and Pool Power Control

In order to study the differences between current control, melt rate control, and pool power control, a simulation of a cracked electrode operating under each of these controllers was performed. A crack impedes heat flow causing material below the crack to heat up more rapidly than normal while material above the crack remains relatively cold. Under constant power conditions, this leads to an increase in melt rate as the melt zone approaches the crack, followed by a rapid decrease as the melt zone passes through the crack. This can be simulated by changing the process efficiency, μ, in Equations (2) and (3) as a function of time. In particular, the simulated process efficiency was increased 20% from its nominal value over a one hour duration, then rapidly decreased to 80% of its nominal value over a 30 second duration, and then slowly increased back to nominal process efficiency over a one hour period. The simulation was performed on a proprietary VAR simulation code developed by Bertram[7] and subsequently modified by one of the authors (Erdmann). The simulation was done for VAR of Alloy 718 with a 42.54 cm (16.75 in) diameter electrode melting into a 50.8 cm (20 in) diameter ingot. The simulation was performed in the quasi-steady state region of the melt such that ingot and electrode height had negligible effect on the result. The nominal process efficiency μ was set at .457 and the power fraction to the pool ε was set at .396. The electrical properties were set at V_{CF} = 21.18 V, R_I = 4.369 x 10^{-4} Ω, R_G = 0 Ω/m, and nominal current I_0 = 5500 A. The nominal gap was set to G = 1 cm. The simulation accounts for helium cooling at a pressure of 5 Torr. The four melt coefficients are $C_{\Delta\Delta}$ = 41.97, $C_{\Delta p}$ = 4.244, $C_{s\Delta}$ = 7.428, and C_{sp} = 1.459.

The current for the three controllers and the resulting melt rate are shown in Figures 2 and 3.

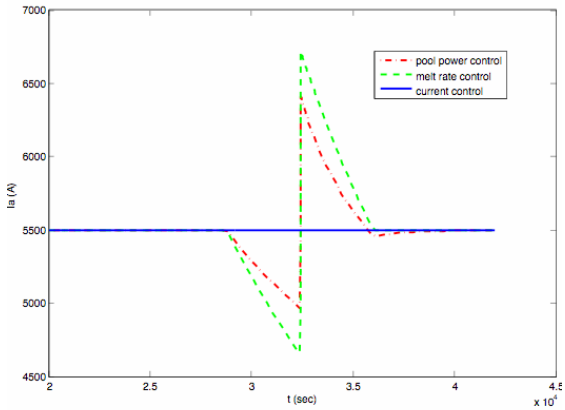

Figure 2: Current profiles for pool power, melt rate and current control from a process efficiency variation starting at 28,800 sec and ending at 36,000 sec.

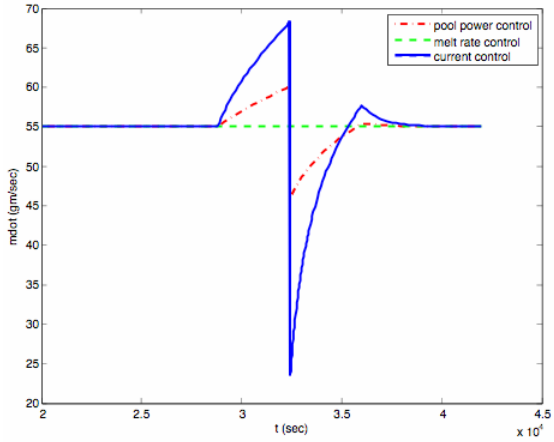

Figure 3: Resulting melt rate profiles for pool power, melt rate and current control from a process efficiency variation starting at 28,800 sec and ending at 36,000 sec.

As can be seen in these two figures for current control the melt rate varies during the transient event while for melt rate control the current varies during the transient event. It is not possible to simultaneously control both the current and the melt rate during this simulated cracked electrode event. Pool power does not attempt to keep either melt rate or current constant during the simulated crack event. But, from Figure 2 note that the commanded current required to keep pool power constant is less than that required to keep melt rate constant. Also, note in Figure 3 that the melt rate deviation that results from pool power control is less than that in current control. In this respect, pool power control requires less control action.

The real interest in VAR process control is the effect on ingot solidification. One way to gauge this effect is to investigate changes in the liquidus pool during the event. Shown in Figure 4 is a plot of total liquidus pool volume during the simulated cracked electrode event. As can be seen in this figure, the pool volume variation is significantly less for pool power control than for either current or melt rate control.

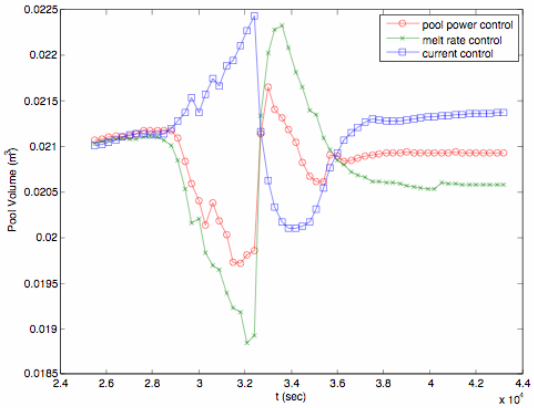

Figure 4: Total liquidus pool volume change for pool power, melt rate and current control from a process efficiency variation starting at 28,800 sec and ending at 36,000 sec.

This effect can also be seen in Figures 5, 6, 7, which are plots of liquidus isotherms for current control, melt rate control, and pool power control, respectively. As can be seen in these figures the variation of the liquidus isotherm is also significantly less for pool power control than for current control and melt rate control.

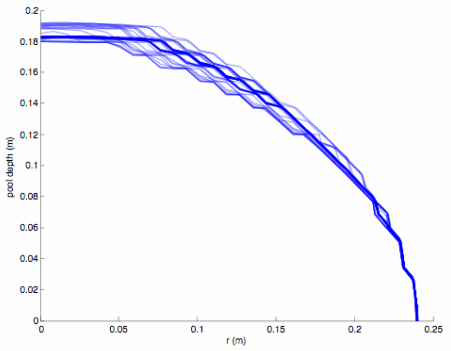

Figure 5: Liquidus isotherm variation for current control control from a process efficiency variation

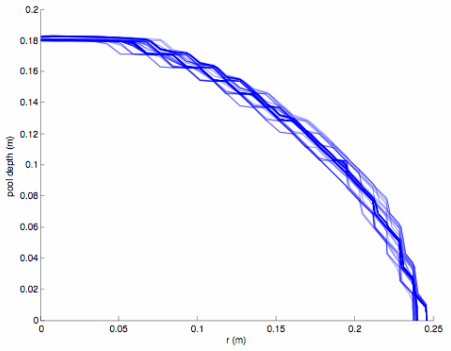

Figure 6: Liquidus isotherm variation for melt rate control control from a process efficiency variation

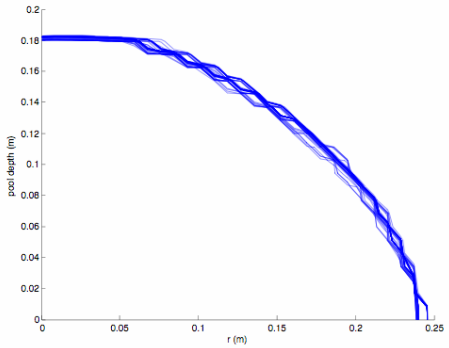

Figure 7: Liquidus isotherm variation for pool power control control from a process efficiency variation

Note that the jagged nature of isotherms in these plots is due to the relatively coarse radial grid (30 points) and the large difference between the liquidus diffusivity (as enhanced by turbulence) and solidus diffusivity.

Figures 5 and 6 can also give insight into the reason for liquidus variations. For current control, Figure 5, the liquidus isotherm variation is most pronounced along the center line of the ingot. This is a direct result of a large amount of melting enthalpy power variation that is deposited prominently in the center of liquidus pool during a melt rate variation. In Figure 6 note that the liquidus isotherm variation is biased towards the outer part of the liquidus pool. This is due to a constant melt enthalpy power input but a varying arc power, which is more evenly distributed across the top of the ingot. Pool power, which has less variation than both current control and melt rate control, can be thought of as the average between the two. The result is less variation in the liquidus pool for pool power control than for current or melt rate control.

IV. Controller Experiments

The pool power controller was tested on the VAR furnace in the MST Foundry at Los Alamos National Laboratory. The test was performed by melting 0.15 m (6 inch) diameter 304SS electrode into 0.22 m (8.5 inch) diameter ingot. The test involved using the controller to melt through welds. For these tests, the arc power fraction was estimated to be 0.3. A 158.5 kg electrode was melted using the pool power controller. The electrode consisted of four pieces butt-welded together as depicted in Figure 8. Each weld extended around the electrode circumference and was performed without filler metal.

Figure 9 shows plots of the voltage and current histories for this test. The positions of the welds are marked in the figure with the exception of Weld 3, which occurred at the very end of melting. That is, the melt was shut off as soon as the weld was encountered. A gap check is also marked in the figure. Figure 10 shows plots of estimated pool power and melt rate. Note the relatively flat power profile and the fluctuations in melt rate in response to the welds. It is clear that the controller is controlling pool power while letting the melt rate vary.

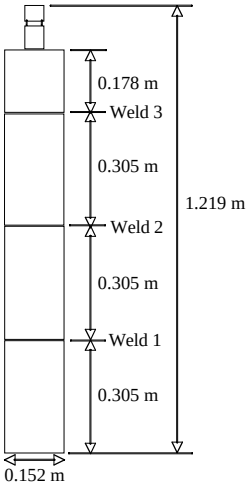

Figure 8: Depiction of the test electrode showing the locations of the three welds. The electrode segments were TIG welded around the electrode circumference.

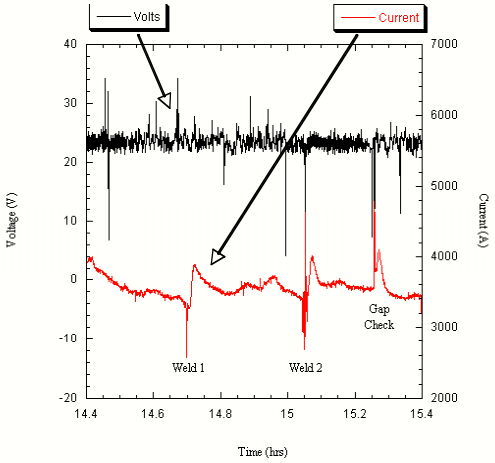

Figure 9: Plots showing voltage and current histories for the pool power control test.

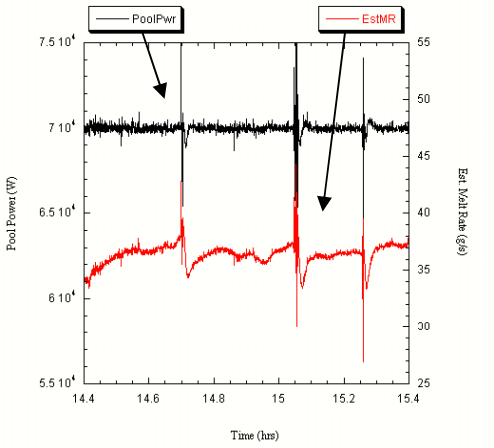

Figure 10: Plots showing estimated pool power and melt rate for the pool power test.

Figure 11 shows load cell and estimated efficiency data. In particular, note the rise in and the rapid drop in efficiency when the electrode face approaches a weld, which has similar effect as a cracked electrode.

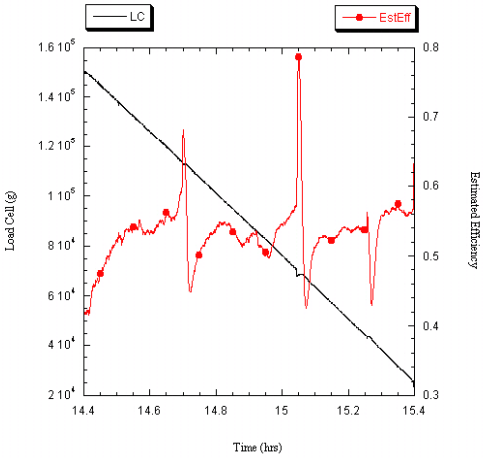

Figure 11: Plots showing load cell data and estimated efficiency for the pool power control test.

The test ingot was sliced lengthwise, polished, and macro-etched. Figure 12 shows the ingot structure. The melt pool profile is visible in the two places where electrode sections fell in when the welds were melted through. Note that the columnar grain structure is maintained through the regions marking the weld effects. Thus, it appears that the electrode fall-in material melted after initially chilling the melt pool. Also visible in the figure is the porosity and rough ingot top due to the fact that the melt was terminated at full power when the third weld was melted though.

Figure 12: Image of sliced and etched ingot from Pool Power control test.

The tests described above demonstrate pool power control under the assumptions used to derive Equation (4). It is clear from the data that the controller held estimated pool power at its reference set-point by manipulating melt rate.

In addition to the pool power control, a separate test was performed with an almost identical welded electrode but using current control rather than pool power control.

Shown in Figure 13 is the result from current control. Note the porosity in the ingot that occurred while the electrode was melting through the welds. As in the pool power test, a portion of the weld fell in, but, in the pool power control, the current quickly rises after the weld event to account for the cold face of the weld and as a result no porosity occurs. This does not happen in current control and porosity results.

Figure 13: Image of siliced and etched ingot from current control test.

Having a large piece of the electrode fall in is certainly a drastic event but the result does demonstrate the robustness of the control scheme and its potential effectiveness for smaller, more realistic disturbances.

A separate melt rate control test with three welds was also conducted. The etched ingot showed no porosity as in pool power control, but at the expense of larger current variation. For example, the current dropped to approximately 2500 A and then peaked at almost 4500 A while melting through weld 1. The commanded current for pool power control briefly dropped to 2500 A but only rose to about 4000 A during the weld 1 event. There is no way of knowing if the welds in the two tests were identical but decreased control effort for pool power is as expected.

V. Conclusion

An alternative method to VAR control was developed and tested by simulation studies and experimental tests of cracked or welded electrodes. Simulation work shows that this new method does a better job of controlling perturbations to the ingot solidification zone as measured by changes in the liquidus pool. This improved control method does not directly control either the current or the melt rate but rather controls the total input power to the top of the ingot pool and for this reason has been termed pool power control.

Acknowledgements

A portion of this work was performed at Sandia National Laboratories which is supported by the United States Department of Energy under contract DE-AC04-94AL85000. Support for this work was also provided by the Specialty Metals Processing Consortium. The authors gratefully acknowledge the cooperation of Los Alamos National Laboratories, Los Alamos, New Mexico in making the tests possible.

References

1. M.C. Flemings, Solidification Processing, McGraw-Hill, New York, NY, p 245,(1974).
2. T. Suzuki, T. Shibata, K. Morita, T. Taketsuru, D.G. Evans and W. Yang, Proc. of The 2001 Int'l Symposium on Liquid Metal Processing And Casting, A. Mitchell and J. Van Den Avyle, ed.'s, American Vacuum Society, Santa Fe, New Mexico, 325-337, (2001).
3. L.A. Bertram, J.A. Brooks, D.G. Evans, A.D. Patel, J.A. Van Den Avyle and D.D. Wegman, Proc. of The 1999 Int'l Symposium on Liquid Metal Processing And Casting, A. Mitchell, L. Ridgway and M. Baldwin, ed.'s, American Vacuum Society, Santa Fe, New Mexico, 156-167, (1999).
4. R.L. Williamson, J.J. Beaman, D.K. Melgaard, G.J. Shelmidine, A.D. Patel, and C.B. Adasczik, Journal of Materials Science, 39, 7161-7168, (2004).
5. R.L. Williamson, J.J. Beaman, D.K. Melgaard, G.J. Shelmidine, R. Morrison, Metallurgical and Materials Transactions B: Process Metallurgy and Materials Processing Science, 35, 101-113, (2004).
6. J.J. Beaman, R. L. Williamson and D. K. Melgaard, Proc. of The 2001 Int'l Symposium on Liquid Metal Processing And Casting, A. Mitchell and J. Van Den Avyle, ed.'s, American Vacuum Society, Santa Fe, New Mexico, pp. 161-174, (2001).
7. L. A. Bertram and F. J. Zanner: *Modeling and Control of Casting And Welding Processes*, S. Kou and R. Mehrabian, ed.'s, TMS, Warrendale, Pennsylvania,, p. 95, (1986)